Simulation of rough wall turbulent channel flow using a parametric forcing approach

A. E. Busse and N. D. Sandham

School of Engineering Sciences, University of Southampton, Highfield, Southampton SO17 1BJ, United Kingdom

E-mail: a.busse@soton.ac.uk, n.sandham@soton.ac.uk

Abstract. The effects of rough walls on turbulent channel flow are simulated by adding a simple forcing term to the Navier-Stokes equations. An extensive parameter study is used to explore the effects of this term on turbulent channel flow. By varying the roughness height parameter and the roughness factor contained in the forcing term it is possible to simulate roughnesses of various strengths ranging from transitionally rough to very rough cases. A good qualitative agreement is found with the results of recent experimental and numerical studies of rough-wall turbulent channel flow for the mean flow statistics. The streamwise velocity shows a very good preservation of the outer layer similarity for both its mean and its fluctuations. The flow structure shows a weakening of the streamwise streaks above the roughness sublayer. Within the roughness sublayer the turbulent structure changes to a more isotropic state, while close to the wall a mixing layer-like turbulent state emerges in extremely rough cases. The roughness force term is a possible candidate for a wall model in large eddy and direct numerical simulations where the small-scale structure of the flow over a rough surface can be neglected.

1. Introduction

In many technical applications as well as in the geophysical context turbulent flows are influenced by the presence of roughnesses on their boundaries (Jiménez, 2004). Rough surfaces can be a side effect of the production process as for cast iron pipes (Langelandsvik *et al.*, 2008) or be made deliberately rough such as in the case of riblets (Karniadakis & Choi, 2003) or superhydrophobic surfaces (Rothstein, 2010). In the geophysical context the size of relevant roughnesses spans several orders of magnitude ranging from sand grains and plant canopies (Finnigan, 2000) to urban roughnesses that can influence the regional climate and local dispersion processes (Arnfield, 2003).

Although it is possible to simulate simple rough surfaces by using body-fitted grids or immersed boundary methods these methods always necessitate a much higher numerical effort than a corresponding numerical simulation of turbulent flow over a smooth surface. As the details of the flow within the rough surface are often of little interest, a simpler method for the simulation of the effects of a rough surface on turbulent flow would be of use.

Modelling of rough surfaces is usually achieved either by modification of boundary conditions or by modification of the Navier-Stokes equations. We take the second approach and add a forcing term to the right hand side of the Navier Stokes equations. The forcing term is formulated using a Cartesian system of coordinates $(\vec{x}_1, \vec{x}_2, \vec{x}_3)$ whose coordinate axes are determined by

the local flow field and the wall geometry. $\vec{x}_1$ indicates the local mean flow direction parallel to the wall[1], $\vec{x}_3$ the wall normal direction; $\vec{x}_2$ completes the coordinate system and is the spanwise direction in the plane of the wall. In the case of a plane channel flow these are simply the streamwise, wall-normal and spanwise directions. The term takes the form $-\alpha_i F_i(x_3, h) u_i |u_i|$ (no summation over i). As no summation is used over i, the streamwise, spanwise and wall-normal velocity components have no additional coupling via the forcing term. We found that this improves the preservation of the outer scaling of the flow significantly (see below).

The roughness forcing term is quadratic in the respective velocity component (reminiscent of the drag force) and the form $\sim (-u_i|u_i|)$ ensures that this term has always a damping effect. The roughness forcing term can be varied using the roughness factor α, the roughness height parameter h and the shape function F. The roughness factor α is related to the density of the roughness elements and their drag coefficient. The roughness height parameter h is used to parametrise the extension of the roughness force term into the flow. The shape function F is used to regulate the influence of the roughness force term with respect to the distance from the wall; far away from the wall the roughness force term should vanish ($F(x_3, h) \to 0$ for $x_3 \gg 0$). Furthermore the shape function should be bounded and positive definite in order to preserve the damping character of the roughness force term. We expect that different shape functions need to be used to simulate the effects of different types of rough surfaces but a direct mapping between a rough surface and a shape function does not exist within the model. In order to make different shape functions comparable the shape functions are normalised by setting their maximum to unity ($\max(F) = 1$). The roughness height parameter is implicitly defined by $h = \int_0^\delta F(z, h) z dz / \int_0^\delta F(z, h) dz$, where δ is the channel half-height.

The proposed forcing term is related to a number of modelling approaches such as the volume averaged Navier-Stokes equations (Whitaker, 1996) which have for example been used in simulations of flows over porous surfaces (Breugem & Boersma, 2005). The shape function shows similarities to the local drag coefficient employed in RANS models (Taylor *et al.*, 1985).

In order to study the effects of the various parameters in the forcing term and to explore its applicability as a wall model an extensive parameter study has been performed for a full range of rough cases ranging from hydraulically smooth to very rough cases.

2. Parameter study

For the parameter study a large number of direct numerical simulations of turbulent channel flow were conducted at a Reynolds number of $Re_\tau = 180$ using a standard second order finite-difference code operating on a staggered grid. The channel had dimensions of $L_x \times L_y \times L_z = 7 \times 3.5 \times 2$ where x denotes the streamwise, y the spanwise and z the wall-normal direction. No-slip boundary conditions were imposed on the upper and lower wall of the channel, periodic boundary conditions in the streamwise and spanwise direction. The grid of size $128 \times 128 \times 128$ was stretched in the wall-normal direction in order to give a higher resolution near the wall ($\Delta z^+_{\min} = 0.75$).

A preliminary study investigating the influence of the different components of the roughness force term showed that the streamwise component has the strongest effect on the flow, leading to an increase in drag. If only the spanwise or wall-normal components of the roughness term act on the flow a small reduction in drag can be observed. The weakest effect was observed for the wall-normal component of the roughness force term. In the main parameter study described in the following the streamwise and spanwise roughness factors were set equal ($\alpha_x = \alpha_y = \alpha$) and the wall-normal roughness factor was set to zero ($\alpha_z = 0$). The same shape function was used in the streamwise and spanwise directions.

[1] The wall is assumed to be at rest; if this is not the case the relative velocity to the wall should be used.

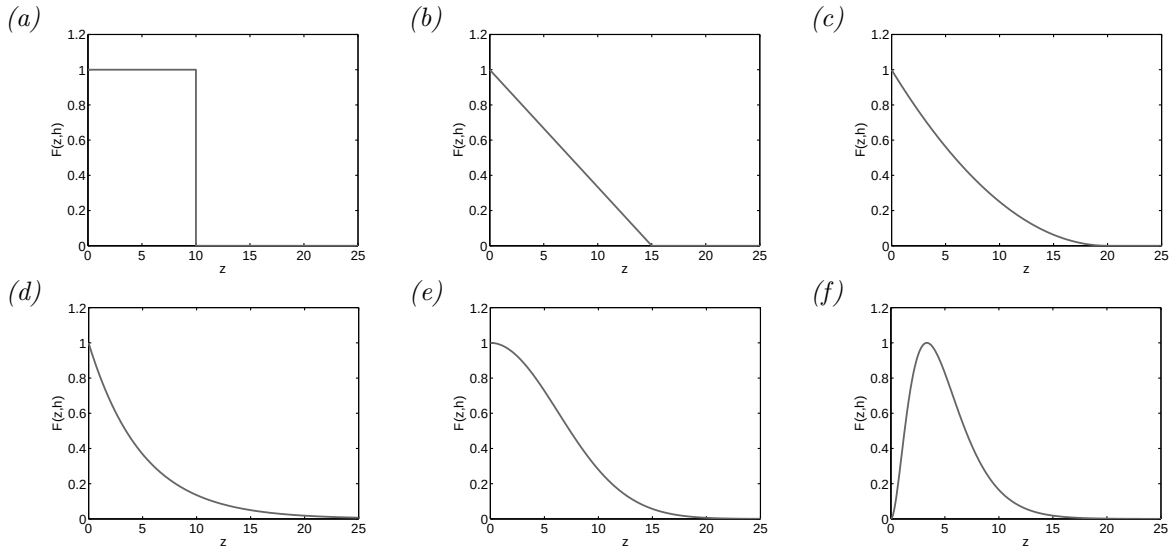

Figure 1. Different types of shape function used to simulate roughnesses in this paper: (a) box, (b) triangular, (c) parabolic, (d) exponentially decaying, (e) Gaussian and (f) orbital shape function. All shape functions illustrated here are based on the same roughness height parameter $h = 5$.

In the main parameter study the roughness height parameter was varied from $h^+ = 2.5$ to $h^+ = 30$ and the roughness factor ranged from $\alpha = 0.04$ to $\alpha = 10$. In most cases either a top-hat like box profile or a Gaussian were used for the shape function. Several other functional forms were tested for the shape function using a subset of the investigated (α, h)-parameter space (see figure 1). In all cases the roughness force term was applied symmetrically to the upper and lower wall of the channel. Standard mean-flow and turbulence statistics have been used to compare the results to experimental and numerical studies of rough-wall turbulent channel flow.

3. Mean flow statistics

The most pertinent effect of rough surfaces on turbulent flows is the downwards shift in the velocity profile ΔU^+, the (Hama) roughness function (see e. g. (Jiménez, 2004)). As expected ΔU^+ increases with increasing roughness factor α as well as with increasing values of the roughness height parameter h^+ (see figure 2 (a) and 3 (a)). Given high enough values for the roughness factor and roughness height the flow can be made fully rough ($\Delta U^+ > 7$). The roughness function also shows a dependence on the roughness shape function which is less pronounced than the dependence on h^+ and α. The difference between the shape functions is clearest for the lowest and highest roughness factors studied here; for the box shape function a saturation can be observed for high roughness factors and high roughness heights whereas for the Gaussian shape function the roughness function continues to increase.

By rescaling the roughness height parameter by a roughness factor and shape function dependent factor $h_{\mathrm{norm}}(F, \alpha)$ it is possible to collapse the curves for the roughness function $\Delta U^+(h)$ in the fully rough region for all roughness factors and shape functions studied so far (see figure 2 (b)). The relationship between the roughness height parameter and the equivalent sand grain roughness is not linear; the equivalent sand grain roughness scales approximately as $k_s \sim h^{2.08}$, although the exact scaling parameter depends on the region used for the fit to the fully rough asymptote. For very high values of ΔU^+ the points start to deviate from the fully rough asymptote. This can be attributed to the moderate Reynolds number used here, which

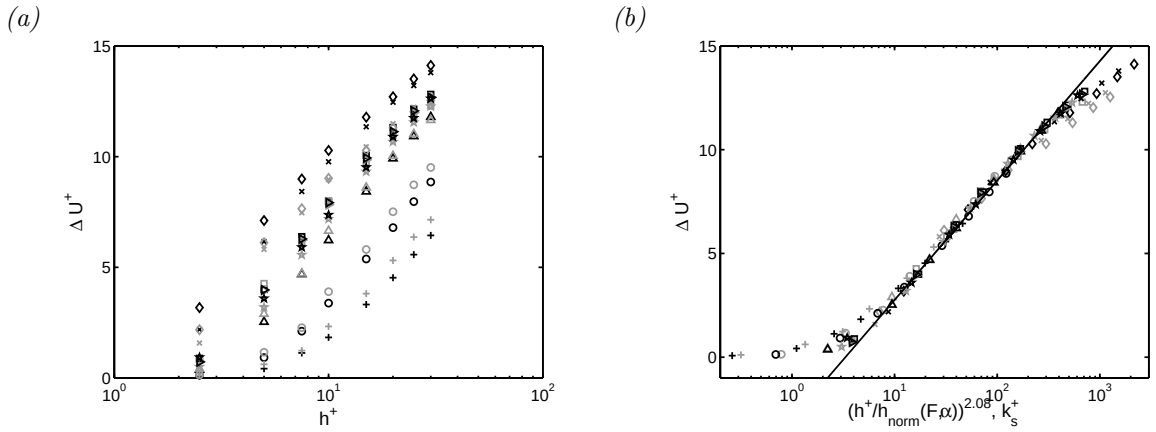

Figure 2. Roughness function for various roughness factors and shape functions: (a) versus roughness height parameter; (b) collapsed data: roughness function versus rescaled height parameter. Symbols and lines: For the Gaussian (black symbols) and box (grey symbols) shape functions results are shown for six different factors (+: $\alpha = 0.04$, ○ : $\alpha = 0.1$, △: $\alpha = 0.4$, □: $\alpha = 1.$, ×: $\alpha = 4$, ♢: $\alpha = 10$). For the four remaining shape functions results are shown for $\alpha = 1$: triangular (black ▷), parabolic (grey ▷), exponentially decaying (black stars), orbital (grey stars). The black line shows the fully rough asymptote.

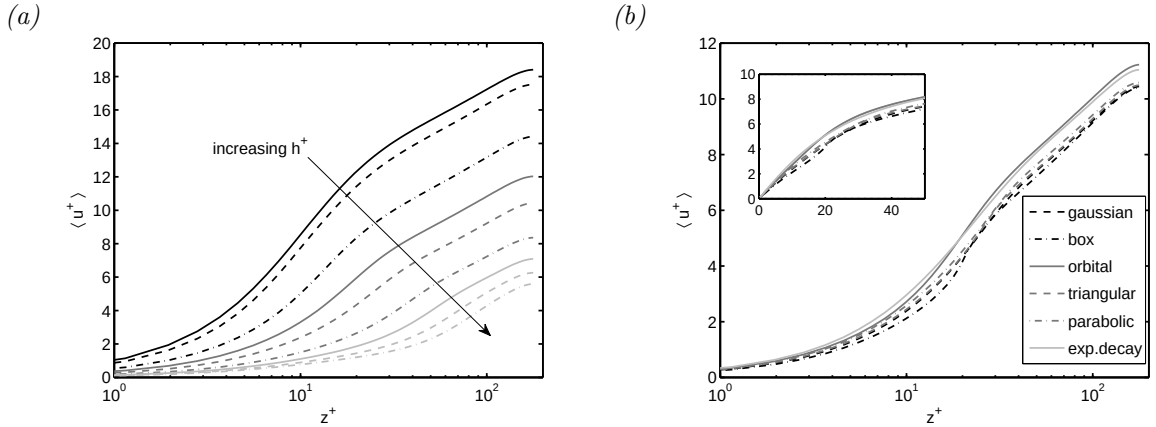

Figure 3. Mean streamwise velocity profile across the channel. (a) Using a Gaussian shape function for a roughness factor of $\alpha = 1.0$ and varying roughness height ($h^+ = 2.5$, 5, 7.5, 10, 15, 20, 25, 30); the black continuous line is showing the smooth-wall reference case. (b) Different shape functions (inset in linear scales) for a roughness factor of $\alpha = 1$ and a roughness height $h^+ = 10$.

leads to a relatively small ratio of the channel height to the friction length scale so that the outer scaling cannot be recovered in very rough cases. In the case of the box profile this departure is amplified by the saturation effects discussed above.

The effects of different shape functions can be observed more clearly in the mean velocity profile (see figure 3 (b)). For all moderately to fully rough cases the box shape function introduces a pronounced inflection point in the mean streamwise velocity profile which is not present for smoother shape functions such as the Gaussian. It is therefore possible to match different types of rough surfaces by using different shape functions. The box profile would be useful in the case of plant canopies where an inflexion point is observed in the mean velocity profile (Finnigan,

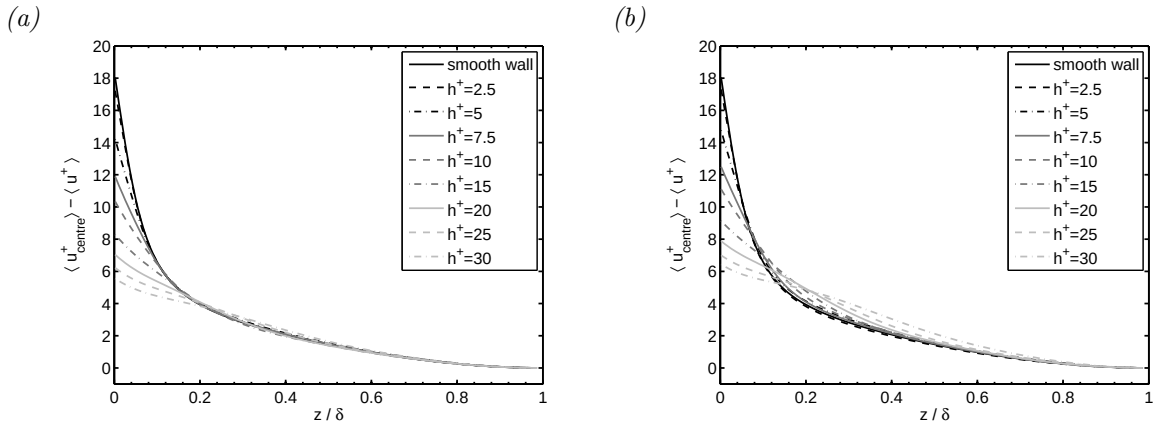

Figure 4. Velocity defect profile across the channel using a Gaussian shape function and a roughness factor $\alpha = 1$ for various roughness heights ($h^+ = 2.5$, 5, 7.5, 10, 15, 20, 25, 30). (a): forcing term $f_i \sim (-|u_i|u_i)$; (b): another possible quadratic form $f_i \sim (-|\vec{u}|u_i)$.

2000) whereas the Gaussian shape function would probably be a good first approximation for roughnesses of a more technical type such as corrugated iron.

The velocity defect profile shows a very good preservation of the outer scaling (as is expected for rough surfaces (Castro, 2007; Birch & Morrison, 2011)) in all but extremely rough cases. This serves also as an example where other possible formulations of a quadratic forcing such as $f_i \sim (-|\vec{u}|u_i)$ show inferior results: for this form of the forcing term the outer scaling is lost even in moderately rough cases (see figure 4).

The fluctuations of the streamwise velocity (not shown) are damped by the presence of the roughness term near the wall whereas the outer layer scaling is preserved in all but very rough cases. This is in agreement with experimental and numerical observations (Krogstad *et al.*, 2005; Amir & Castro, 2011). The fluctuations of the spanwise and wall-normal velocity component are also damped but to a considerably smaller degree than the streamwise velocity component so that the ratio of wall-normal to streamwise velocity fluctuations increases with increasing roughness height and roughness factor. In flow over roughness elements eddies are generated on the scale of the roughness elements and below. This injection of additional turbulent kinetic energy is an effect the model cannot reproduce. Therefore the observed lower level of spanwise and wall-normal velocity fluctuations compared to experimental observations is not unexpected.

4. Flow structure

Rough surfaces have a strong influence on the structure of turbulence in the near wall region. The changes in the structure of the velocity field will be influenced by the particular geometry of the rough surface. A strong preferential direction in the arrangement of the roughness elements (such as for riblets or grooves) will be reflected in the structure of the velocity field. In the case of approximately isotropic rough surfaces (which should correspond closest to the $\alpha_1 = \alpha_2$ case studied here) a decrease of the streamwise correlation of the velocity field is observed (Bhaganagar *et al.*, 2004). For surfaces with spanwise grooves a strong increase in the spanwise correlation is observed (Leonardi *et al.*, 2004; DeMarchis *et al.*, 2010); however this might be a feature that is introduced or enhanced by the presence of the grooves.

In the simulations with the roughness force term similar observations for the change in the flow structure can be made. In order to give an overview over the change in the structure of the streamwise velocity field at various distances from the wall the correlation length scales of the streamwise velocity component in the streamwise ($L_{u,xx}$) and spanwise ($L_{u,yy}$) direction

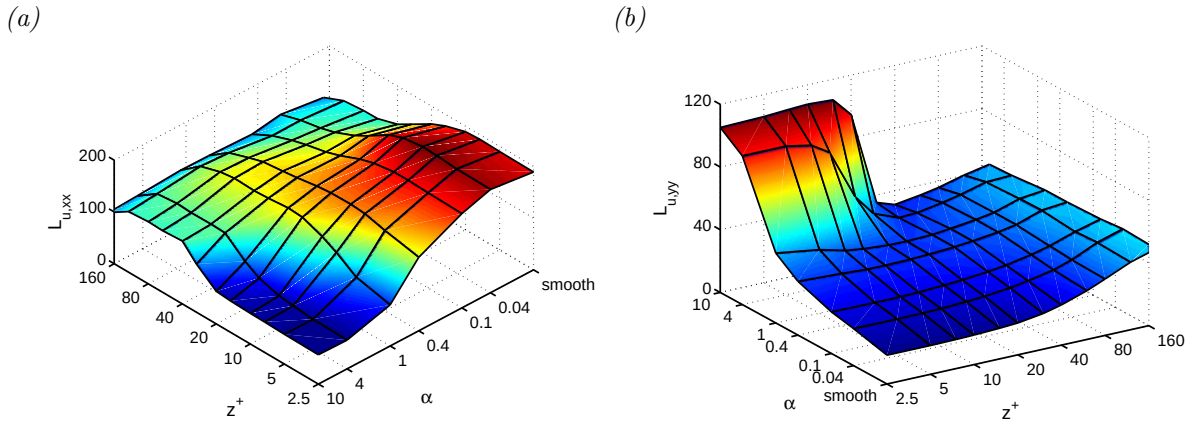

Figure 5. Correlation length scales for the streamwise velocity component for various roughness factors and distances from the wall for a roughness height parameter $h^+ = 20$ using a Gaussian shape function: (a) streamwise correlation length scale $L_{u,xx}$; (b) spanwise correlation length scale $L_{u,yy}$.

are shown in figure 5. The correlation length scales are based on a $1/e$ measure[2] that is $L_{u,xx} = \min\{\Delta x | R_{u,xx}(\Delta x) \leq 1/e\}$ where $R_{u,xx}(\Delta x)$ is the streamwise two-point correlation function of the streamwise velocity component ($L_{u,yy}$ is defined in an analogous manner). When the correlation length above the roughness sublayer (at $z^+ \approx 2h^+$) is considered, a decrease of the streamwise correlation length $L_{u,xx}$ compared to the smooth wall reference case can be observed. This decrease increases with increasing roughness factor α. The spanwise correlation length shows a small increase compared to the smooth wall reference case. This indicates that the streaks above the roughness sublayer are shortened compared to the streaks over a smooth wall. Far away from the wall towards the middle of the channel the correlation length scales are similar to the smooth wall reference case and the structure of the velocity field in the centre of the channel appears to be largely unchanged by the presence of the roughness force term.

Within the roughness sublayer (below $z^+ = 2h^+$) more striking changes in the flow structure can be observed. For high roughness factors a very pronounced decrease in the streamwise correlation length can be observed together with a strong increase of the spanwise correlation length. The consequences for the structure of the velocity field can be illustrated by the ratio of these two length scales (see figure 6 (a)): In the smooth wall reference case (as well as in cases corresponding to small values of the roughness function) a high aspect ratio $L_{u,xx} \gg L_{u,yy}$ is measured which indicates the presence of long streamwise streaks in the velocity field. The aspect ratio is decreased by the presence of the roughness term[3]. For cases corresponding to very large values of ΔU^+, $L_{u,yy}$ can become larger than $L_{u,xx}$, showing that spanwise structures start to dominate the streamwise velocity field.

The loss of the quasi one-dimensional streaky structure in the roughness sublayer is also reflected in the anisotropy invariant map of the Reynolds stress anisotropy tensor. The Reynolds stress anisotropy tensor

$$b_{ij} = \frac{\langle u_i' u_j' \rangle}{\sum_{k=1}^{3} u_k' u_k'} - \frac{1}{3}\delta_{ij} \tag{1}$$

[2] This measure for the correlation length scale was chosen as it is defined in all cases studied here and is less affected by the finite domain size than other measures such as the integral length scale.

[3] A reduction of the ratio of the streamwise to the spanwise correlation length of the streamwise velocity within the roughness sublayer has also been observed in the experiments of Reynolds & Castro (2008) for flow over staggered cube roughnesses.

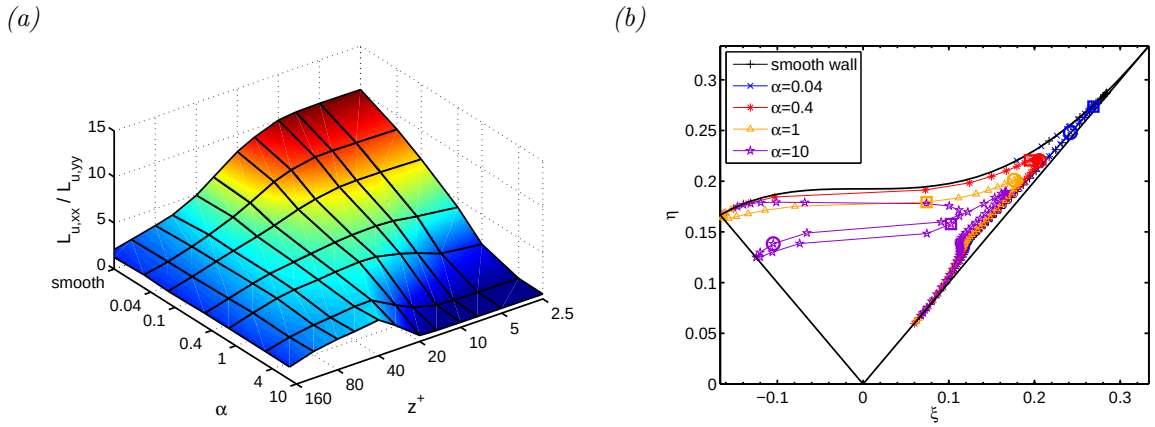

Figure 6. (a) Ratio of streamwise to spanwise correlation length scale of the streamwise velocity component for various roughness factors and distances from the wall for a roughness height parameter $h^+ = 20$ using a Gaussian shape function. (b) Anisotropy invariant map of the Reynolds stress tensor for various roughness amplitudes for a roughness height parameter $h^+ = 10$ using a Gaussian shape function; the thin black lines indicate the Lumley triangle.

is a standard measure for the anisotropy of the turbulent velocity fluctuations (Pope, 2000; Simonsen & Krogstad, 2005). The anisotropy invariant map (Lumley, 1978) is constructed using the second and third principal invariants of this tensor: $\eta = \sqrt{\frac{1}{6}\sum_{i,j} b_{ij}b_{ji}}$ indicates the degree of anisotropy, and $\xi = \sqrt[3]{\frac{1}{6}\sum_{i,j,k} b_{ij}b_{jk}b_{ki}}$ the type of anisotropy. The Lumley triangle encompasses all possible turbulent states on the anisotropy invariant map (see figure 6 (b)). In the smooth wall case the turbulence is of two-component type close to the wall. The anisotropy increases close to the wall while traversing the viscous sublayer and reaches a peak around $z^+ \approx 8$. Further away from the wall it follows closely the right edge of the Lumley triangle, being close to a rod-like axisymmetric state of turbulence. The degree of anisotropy decreases with increasing distance from the channel wall. In the cases with roughness the path across the anisotropy map shows increasing deviations from the path in the smooth wall reference case for increasing h^+ and α. The first difference is visible even for small values of the roughness parameters. The path across the anisotropy map starts in the left half of the anisotropy invariant map near the left upper edge of the Lumley triangle, indicating an approximately disk-like axisymmetric state near the wall. This is due to the fact that the streamwise velocity fluctuations are damped much more by the roughness force term than the fluctuations of the spanwise velocity component. Further away from the wall the path eventually merges with that of the smooth wall reference case, indicating that the roughness term does not significantly change the anisotropy of the Reynolds stresses in the outer layer of the flow. Overall the maximum anisotropy attained, i.e. the peak value of η, is significantly lower than in the smooth wall reference case. These observations follow similar trends as observed in experimental and numerical studies of flow over rough surfaces (Antonia & Krogstad, 2001; Smalley *et al.*, 2002; Ashrafian & Andersson, 2006; DeMarchis *et al.*, 2010). With increasing values of the roughness parameters h^+ and α the path stays longer in the left hand side of the anisotropy invariant map, in some cases crossing the map twice. In the roughness sublayer, which is strongly affected by the roughness force term, the turbulence is no longer of a rod-like type as for a standard channel flow but rather of disk-like type as is observed for a turbulent mixing layer (Bell & Mehta, 1990; Pope, 2000).

5. Conclusions

By adding a simple body force term to the Navier-Stokes equations it is possible to model many aspects of flow over rough surfaces without incurring the numerical cost of resolving the flow over a complex surface geometry. The degree of roughness can be varied from hydraulically smooth to very rough by adjusting the parameters contained in the force term. A non-linear relationship could be established between the roughness height parameter and the equivalent sand grain roughness. The roughness force term did not impair the outer scaling of the mean streamwise velocity profile unlike another possible quadratic formulation of the term.

The flow structure showed a change towards a more isotropic form of turbulence in the roughness sublayer regarding the correlation of the streamwise velocity component as well as the anisotropy of the Reynolds stresses, in agreement with recent experimental and numerical observations. In some very rough cases not only were the streamwise streaks in the velocity field damped, but new spanwise structures emerged in the flow field.

Some aspects of flows over rough walls cannot be reproduced by the force term; this is due to the fact that the shedding of eddies by the roughness elements is not resolved by the model. Therefore the level of wall-normal velocity fluctuations tends to be too low and there is no increase of small scale turbulent structures on the scale of the roughness elements and below. As the model is ab initio only applicable in situations where the exact small scale structure of the flow is negligible this seems to be a modest price to pay. For practical applications as a rough-wall model a calibration of this model against experiments or against direct numerical simulations in which the full detail of the surface is resolved would be necessary. The two main parameters would be the roughness factor and the roughness height with some additional fine-tuning provided by the roughness shape function.

References

Amir, M. & Castro, I. P. 2011 Turbulence in rough-wall boundary layers: universality issues. *Exp. Fluids* .

Antonia, R. A. & Krogstad, P.-A. 2001 Turbulence structure in boundary layers over different types of surface roughness. *Fluid Dyn. Res.* **28**, 139–157.

Arnfield, A. J. 2003 Two decades of urban climate research: A review of turbulence, exchanges of energy and water, and the urban heat island. *Int. J. Climatol.* **23** (1), 1–26.

Ashrafian, A. & Andersson, H. I. 2006 The structure of turbulence in a rod-roughened channel. *Int. J. Heat Fluid Fl.* **27**, 65–79.

Bell, J. H. & Mehta, R. D. 1990 Development of a two-stream mixing layer from tripped and untripped boundary layers. *AIAA J.* **28**, 2034–2042.

Bhaganagar, K., Kim, J. & Coleman, G. 2004 Effect of roughness on wall-bounded turbulence. *Flow Turbul. Combust.* **72**, 463–492.

Birch, D. M. & Morrison, J. F. 2011 Similarity of the streamwise velocity component in very-rough-wall channel flow. *J. Fluid Mech.* **668**, 174–201.

Breugem, W. P. & Boersma, B. J. 2005 Direct numerical simulations of turbulent flow over a permeable wall using a direct and a continuum approach. *Phys. Fluids* **17**, 025103.

Castro, I. P. 2007 Rough-wall boundary layers: mean flow universality. *J. Fluid Mech.* **585**, 469–485.

DeMarchis, M., Napoli, E. & Armenio, V. 2010 Turbulence structure over irregular rough surfaces. *J. Turbulen.* **11** (3), 1–32.

Finnigan, J. 2000 Turbulence in plant canopies. *Annu. Rev. Fluid Mech.* **32**, 519–571.

Jiménez, J. 2004 Turbulent flow over rough walls. *Annu. Rev. Fluid Mech.* **36**, 173–96.

Karniadakis, G. E. & Choi, K.-S. 2003 Mechanisms on transverse motions in turbulent wall flows. *Annu. Rev. Fluid Mech.* **35**, 45–62.

Krogstad, P.-A., Andersson, H. I., Bakken, O. M. & Ashrafian, A. 2005 An experimental and numerical study of channel flow with rough walls. *J. Fluid Mech.* **530**, 327–352.

Langelandsvik, L. I., Kunkel, G. J. & Smits, A. J. 2008 Flow in a commercial steel pipe. *J. Fluid Mech.* **595**, 323–339.

Leonardi, S., Orlandi, P., Djenidi, L. & Antonia, R. A. 2004 Structure of turbulent channel flow with square bars on one wall. *Int. J. Heat Fluid Flow* **25**, 384–392.

Lumley, J. L. 1978 Computational modeling of turbulent flows. *Adv. Appl. Mech.* **18**, 123–176.

Pope, Stephen B. 2000 *Turbulent Flows*. Cambridge University Press.

Reynolds, R. T. & Castro, I. P. 2008 Measurements in an urban-type boundary layer. *Exp. Fluids* **45**, 141–156.

Rothstein, J. P. 2010 Slip on superhydrophobic surfaces. *Annu. Rev. Fluid Mech.* **42**, 89–109.

Simonsen, A. J. & Krogstad, P. A. 2005 Turbulent stress invariant analysis: Clarification of existing terminology. *Phys. Fluids* **17**, 088103.

Smalley, R. J., Leonardi, S., Antonia, R. A., Djenidi, L. & Orlandi, P. 2002 Reynolds stress anisotropy of turbulent rough wall layers. *Experiments in Fluids* **33**, 31–37.

Taylor, R. P., Coleman, H. W. & Hodge, B. K. 1985 Predicition of turbulent rough-wall skin friction using a discrete element approach. *J. Fluids Engin.* **107**, 251–257.

Whitaker, S. 1996 The Forchheimer equation: a theoretical development. *Transp. Porous Media* **25**, 27.